Citation: CPT Pharmacometrics Syst. Pharmacol. (2017) 6, 814–822; doi:10.1002/psp4.12252

ORIGINAL ARTICLE

Development of an Adult Physiologically Based Pharmacokinetic Model of Solithromycin in Plasma and Epithelial Lining Fluid

Sara N. Salerno[1], Andrea Edginton[2], Michael Cohen-Wolkowiez[3,4], Christoph P. Hornik[1,3,4], Kevin M. Watt[3,4], Brian D. Jamieson[5] and Daniel Gonzalez[1]*

Solithromycin is a fluoroketolide antibiotic under investigation for community-acquired bacterial pneumonia (CABP). We developed a whole-body physiologically based pharmacokinetic (PBPK) model for solithromycin in adults using PK-Sim and MoBi version 6.2, which incorporated time-dependent CYP3A4 auto-inhibition. The model was developed and evaluated using plasma and epithelial lining fluid (ELF) concentration data from 100 healthy subjects and 22 patients with CABP (1,966 plasma, 30 ELF samples). We performed population simulations and calculated the number of observations falling outside the 90% prediction interval. For the oral regimen (800 mg on day 1 and 400 mg daily on days 2–5) that was evaluated in phase III studies, 11% and 23% of observations from healthy adults fell outside the 90% prediction interval for plasma and ELF, respectively. This regimen should be effective because ≥97% of simulated adults achieved area under the concentration vs. time curve (AUC) to minimum inhibitory concentration ratios associated with a $\log_{10}$ colony forming unit reduction in ELF.
CPT Pharmacometrics Syst. Pharmacol. (2017) **6**, 814–822; doi:10.1002/psp4.12252; published online 25 October 2017.

Study Highlights

WHAT IS THE CURRENT KNOWLEDGE ON THE TOPIC?

☑ Solithromycin is a new fluoroketolide antibiotic in development for CABP with activity against macrolide-resistant pathogens.

WHAT QUESTION DID THIS STUDY ADDRESS?

☑ The study sought to develop a whole-body PBPK model for solithromycin that incorporated time-dependent inhibition for CYP3A4 and dose-dependent absorption.

WHAT THIS STUDY ADDS TO OUR KNOWLEDGE

☑ The oral dosing regimen evaluated in phase III clinical trials should be effective because ≥97% of simulated adults achieved AUC to minimum inhibitory concentration ratios associated with a $\log_{10}$ colony forming unit reduction in ELF.

HOW MIGHT THIS CHANGE DRUG DISCOVERY, DEVELOPMENT, AND/OR THERAPEUTICS?

☑ This PBPK model can be applied to predict solithromycin exposure in children and other special populations and it serves as a framework for other drugs with time-dependent inhibition and ELF data.

Community-acquired bacterial pneumonia (CABP) causes significant morbidity and mortality, and resistance to pathogens causing CABP is a worldwide problem.[1,2] Nationally, macrolide-resistant *Streptococcus pneumoniae* has increased from 23% in 1999 to 34% in 2012.[2] Therefore, there is an urgent need to develop new antibiotics for the treatment of CABP. Solithromycin is a fluoroketolide antibiotic with oral (capsule and suspension) and i.v. formulations under investigation for the treatment of CABP and uncomplicated urogenital gonorrhea. It is a bactericidal antibiotic that has activity against macrolide-resistant bacteria due to interactions with three distinct sites on the bacterial ribosome.[3] Solithromycin was efficacious and noninferior to moxifloxacin in two adult phase III CABP studies.[4,5] The first study compared oral solithromycin (800 mg on day 1 followed by 400 mg daily on days 2–5) with 400 mg oral moxifloxacin,[4] and the second study compared switching from i.v. to oral solithromycin (400 mg i.v. to 800 mg oral on the first day followed by 400 mg p.o. daily) vs. i.v. to oral administration of moxifloxacin (400 mg).[5]

Solithromycin is metabolized primarily by cytochrome P450 3A4 (CYP3A4), and its metabolites are primarily excreted through the biliary/fecal route of elimination. Solithromycin undergoes mechanism-based (time-dependent) inhibition of CYP3A4, so it inhibits its own metabolism and accumulation can occur. In a dose escalation study in healthy subjects administered capsules daily for 7 days, the area under the solithromycin plasma concentration vs. time curve from 0–24 hours (AUC_{0-24}) was higher on day 7 compared to day 1 with mean accumulation indexes of 3.02, 5.22, and 7.76 following 200 mg, 400 mg, and 600 mg, respectively.[6] Solithromycin is also a substrate of

[1]Division of Pharmacotherapy and Experimental Therapeutics, UNC Eshelman School of Pharmacy, The University of North Carolina at Chapel Hill, Chapel Hill, North Carolina, USA; [2]School of Pharmacy, University of Waterloo, Kitchener, Ontario, Canada; [3]Department of Pediatrics, Duke University Medical Center, Durham, North Carolina, USA; [4]Duke Clinical Research Institute, Duke University Medical Center, Durham, North Carolina, USA; [5]Cempra Inc, Chapel Hill, North Carolina, USA. *Correspondence: D Gonzalez (daniel.gonzalez@unc.edu)
Received 22 June 2017; accepted 4 September 2017; published online on 25 October 2017. doi:10.1002/psp4.12252

Table 1 Solithromycin parameters used for the physiologically based pharmacokinetic model

Parameter	Initial value	Final value	Source
Molecular weight (g/mol)	845.01	845.01	Sponsor data on file
Log P	4.25	3.75	Parameter optimization
pKa	9.44	9.44	Sponsor data on file
Compound type	Diprotic base	Diprotic base	Sponsor data on file
fu	0.22	0.22	Sponsor data on file
Intestinal permeability (transcellular) (10^{-5} cm/min)	0.61	2.42	Parameter optimization
V_{max} P-gp (μmol/L/min)	N/A	2.08	Parameter optimization
K_m P-gp (μM)	N/A	0.95	Parameter optimization
K_m CYP3A4 (μM)	58	58	Vieira *et al*.[19]
V_{max} CYP3A4 (μmol/L/min)	N/A	450	Parameter optimization
K_I CYP3A4 (μM)	0.045	0.045	Sponsor data on file
k_{inact} CYP3A4 (min^{-1})	0.022	0.022	Sponsor data on file

f_u, unbound fraction; K_I, intrinsic inhibition constant; K_{inact}, maximal inactivation rate constant; K_m, Michaelis-Menten constant; Log P, logarithmic of drug permeability; N/A, not available; P-gp, p-glycoprotein; pKa, negative logarithmic of the acid dissociation constant; V_{max}, maximal rate of metabolism.

P-glycoprotein (P-gp), and the mean binding to human plasma, serum albumin, and α_1-acid glycoprotein measured by equilibrium dialysis was 78%, 50%, and 7%, respectively. A population pharmacokinetic (PK) model was developed using adult solithromycin data that included a capacity-limited first-pass effect to describe the observed increased bioavailability with dose.[7] The change in bioavailability with dose is hypothesized to be due to inhibition of P-gp efflux on the intestinal epithelial cells and/or inhibition of first-pass metabolism by CYP3A4 in the intestines and liver. In addition, the delay in the onset of clearance inhibition indicated by the i.v. data was accounted for in the population PK model via an effect compartment.[7]

Solithromycin distributes extensively into the lungs, and has demonstrated efficacy in adults with CABP. In 30 healthy adult subjects who received 400 mg (capsules) daily for 5 days, the mean ratios of epithelial lining fluid (ELF) and alveolar macrophages (AMs) to plasma concentrations ranged from 8.8–14.0 and 132–345, respectively.[8] In a neutropenic murine-lung infection model, the ELF and unbound plasma AUC_{0-24} to minimum inhibitory concentration ratios (AUC_{0-24}/MIC) were associated with efficacy. AUC_{0-24}/MIC ratios in ELF and unbound plasma of 1.26 and 1.65 were associated with bacterial stasis and 15.1 and 6.31 with a 1-$\log_{10}$ colony forming unit reduction, respectively.[9] The objective of this study was to develop a physiologically based pharmacokinetic (PBPK) model leveraging solithromycin clinical trial data and available *in vitro* data for parameter optimization to accurately predict time-dependent CYP3A4 inhibition and concentrations in ELF, and then to simulate exposure following administration of an oral dosing regimen evaluated in phase III trials.

METHODS

Clinical trial data

The clinical trial data used for model optimization and evaluation included 100 healthy subjects from phase I studies and 22 patients with CABP from a phase II study (**Supplementary Table S1**).[6,8,10] The i.v. regimens included 400 mg daily for 7 days and a single dose of 800 mg (sponsor data (Cempra, Chapel Hill, NC) on file). Multiple dose oral regimens included 200 mg, 400 mg, and 600 mg capsules daily for 7 days[6]; 800 mg capsules on day 1 followed by 400 mg capsules daily on days 2–5 (sponsor data (Cempra) on file); and 400 mg daily for 5 days.[8] All clinical studies were conducted in accordance with the ethical standards of the institutional and/or national research committee and with the Helsinki Declaration. Solithromycin concentrations measured in 1,966 plasma samples and 30 ELF samples were used for this analysis. There were 100 samples below the limit of quantification (BLQ = 10 ng/mL), which, for the purpose of parameter optimization, the first BLQ in a trailing series was set to the lower limit of quantification divided by 2 (i.e., 5 ng/mL) with subsequent BLQs ignored.

Initial model development

We developed a whole-body PBPK model for solithromycin in adults using the software PK-Sim and MoBi (version 6.2; Bayer Technology Services, Leverkusen, Germany). The PBPK model for solithromycin was constructed using *in vitro* data and physicochemical properties (**Table 1**). A mean individual was used in initial model development based on study CE01–121: a 44.7-year-old black American man with a weight of 85.6 kg and a height of 180.9 cm. The processes that define solithromycin disposition were incorporated within the initial model, including glomerular filtration, CYP3A4 metabolism, time-dependent inhibition (TDI), P-gp transport, and enterohepatic recycling. The relative organ contributions of P-gp and CYP3A4 were taken from the built-in database query, thereby allowing one set of kinetic parameters to be used in all organs.[11] Further parameterizations of these processes are described below.

Modeling CYP3A4 metabolism and TDI

The kinetic parameters for TDI are the maximal inactivation rate constant (K_{inact}) and the intrinsic inhibition constant (K_I), which describes the concentration at which the inactivation rate is half-maximal. To model TDI in PK-Sim, we selected irreversible inhibition/mechanism-based inactivation, and added K_{inact} and K_I parameters for CYP3A4. The K_{inact} and K_I were determined by measuring the formation

of 1′-hydroxymidazolam in human liver microsomes incubated with nicotinamide adenine dinucleotide phosphate (NADPH), solithromycin, and midazolam (sponsor data (Cempra) on file).

The model for mechanism-based inactivation can be described below where EI is the new complex formed by the enzyme and inhibitor, EI' is a reactive species that forms a covalent complex (E_{inact}) with the enzyme, and K_1, K_{-1}, K_2, K_3, and K_4 are the rate constants for formation and degradation of the EI complex, formation of the EI' complex, release of the enzyme with formation of product, and formation of the E_{inact} complex, respectively:

$$\text{Enzyme} + \text{Inhibitor} \underset{K_{-1}}{\overset{K_1}{\rightleftharpoons}} \text{EI} \xrightarrow{K_2} \text{EI}' \xrightarrow{K_4} E_{inact}$$
$$\text{EI} \xrightarrow{K_3} \text{Enzyme} + \text{Product}$$

The equations for K_{inact} and K_I are shown in Eqs. 1 and 2. The implementation for enzyme turnover (dEcat(T)/dt) is described in Eq. 3, where K_{deg} is the degradation constant, E_0 is the initial enzyme concentration, T is time, I is the inhibitor concentration, and E_{cat} is the catalytic enzyme activity.

$$k_{inact} = \frac{K_2 * K_4}{K_2 + K_3 + K_4} \quad (1)$$

$$K_I = \left(\frac{K_{-1} + K_2}{K_1}\right) * \left(\frac{K_3 + K_4}{K_2 + K_3 + K_4}\right) \quad (2)$$

$$\frac{dE_{cat}(T)}{dT} = K_{deg} * E_0 - \left(K_{deg} + \frac{K_{inact} * I(T)}{K_I + I(T)}\right) * E_{cat}(T) \quad (3)$$

We used the software default degradation half-lives for CYP3A4 in the liver and intestines, which were 37 hours and 23 hours corresponding to a K_{deg} of 0.019 $hour^{-1}$ and 0.03 $hour^{-1}$, respectively. These default values are similar to estimates reported in the literature from studies in the rat, Caco-2 cells, human hepatocyte, and liver slices: 14–44 hours and 12–33 hours for the degradation half-life in the liver and intestines, respectively.[12–18] The relative organ contributions to CYP3A4-mediated clearance were taken from the built-in database query using the reverse transcription polymerase chain expression levels for CYP3A4, as previously described.[11] Because there was no *in vitro* or published data available for solithromycin, dose-dependent saturation was modeled using the CYP3A4 Michaelis-Menten constant (K_m) for telithromycin, a third-generation macrolide of the ketolide class, obtained from a previously published PBPK model[19] while optimizing CYP3A4 maximal rate of metabolism (V_{max}) for solithromycin.

Incorporating P-gp transport

Bidirectional permeability studies in Caco-2 cells demonstrated that solithromycin is a substrate for P-gp transport because bidirectional permeability was higher in the basolateral to apical direction compared to the apical to basolateral direction. The highest observed efflux ratio was ~8.28, which decreased close to unity in the presence of inhibitors (10 μM PSC833 and 60 μM verapamil), indicating that solithromycin is a substrate of P-gp. Furthermore, the observed efflux ratios decreased with increasing doses of solithromycin (8.28, 6.65, and 2.48 at 0.3, 1, and 10 μM of solithromycin, respectively) indicating saturable kinetics. However, because these studies only evaluated three concentrations of solithromycin at four time points, the K_m and V_{max} for P-gp transport could not be determined (sponsor data (Cempra) on file). Thus, P-gp K_m and V_{max} were parameterized through optimization and these values were applied to each organ expressing P-gp. The relative expression levels for P-gp in each organ were taken from the built-in database query using the reverse transcription polymerase chain reaction relative values, as previously described.[11] Because P-gp effluxes to bile, gallbladder emptying was enabled, thus allowing solithromycin to undergo enterohepatic recirculation.

Solithromycin is expected to be secreted into the urine through tubular secretion via P-gp because this transporter is highly expressed in the kidneys.[11] The mean cumulative amount of solithromycin equivalent dose excreted in urine was ~88.9 mg equivalents (11.4% of the dose) after 24 hours and 106 mg equivalents (13.6% of the dose) after 48 hours (sponsor data (Cempra) on file). Because renal plasma clearance is greater than what can be contributed from glomerular filtration alone, maximal glomerular filtration was assumed (glomerular filtration rate * fraction unbound in plasma ($f_{u,p}$)). The predicted vs. observed fraction excreted unchanged in urine was compared as one way to assess the appropriateness of P-gp K_m and V_{max} optimization.

Absorption modeling

We used the built-in database query in PK-Sim to allow a single set of kinetic parameters (K_m/V_{max} and K_I/K_{inact} for CYP3A4) to be used in each organ expressing the protein thereby allowing for gut and liver metabolism. Absorption was modeled with a Weibull distribution, and optimization of the observed oral data was performed to obtain a dissolution time of 30 minutes and a dissolution shape of 1. The Weibull function can describe almost any type of dissolution curve and it is particularly advantageous when the mechanism of release underlying dissolution is unknown.[20] Intestinal transcellular permeability is estimated in PK-Sim. The appropriateness of the estimated value was assessed during the optimization procedure.

Parameter optimization

Initially, using i.v. data only, CYP3A4 V_{max} and P-gp K_m and V_{max} were optimized using observed data from clinical trials. These initial values were then used as starting values for a more comprehensive optimization using both the i.v. and oral data where CYP3A4 V_{max}, P-gp K_m and V_{max}, and intestinal permeability were optimized. Based on this optimization, it was evident that the model simulations underestimated the observed oral data from clinical trials, particularly around the time of the maximum concentration (C_{max}). Modification of intestinal permeability could not account for this underestimation in C_{max}. As such, the final optimization focused on CYP3A4 V_{max}, P-gp K_m and V_{max},

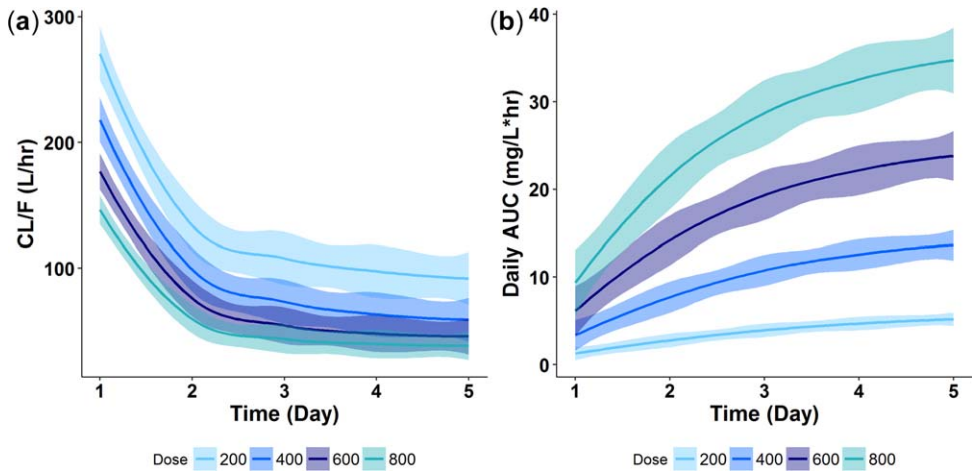

Figure 1 Changes in clearance (**a**) and area under the solithromycin plasma concentration vs. time curve (AUC) from 0–24 hours (**b**) by days of solithromycin treatment. CL/F is the clearance following oral administration. The solid line is the average and the shaded band is the 95% confidence interval for 100 simulated healthy adult subjects for each dose.

lipophilicity, and intestinal permeability. Distribution volume, a major contributor of C_{max}, is dependent on tissue:plasma partition coefficients and lipophilicity using the Berezhkovskiy algorithm.[21] The mean individual was used for all optimization and a Monte Carlo algorithm. The final parameter estimates are shown in **Table 1**. A local sensitivity analysis was also performed to determine which input parameters had the most impact on the simulated output (**Supplementary Information S1**).

Simulations and model validation

We performed simulations for 100 simulated subjects using a black American population with demographics from study CE01–102 for healthy subjects and study CE01–200 for patients with CABP (**Supplementary Table S1**). Population variability for CYP3A4 content, CYP3A4 half-life in the liver and intestines, and P-gp content was introduced using a normal distribution with coefficients of variation of 95%,[22] 60%,[23,24] 24%,[15] and 65%,[25] respectively. We also added variability for $f_{u,p}$ using a normal distribution with a coefficient of variation of 25% to capture the variability in protein binding observed following a phase I study (sponsor data (Cempra) on file). To evaluate the model, we calculated the number of observations from clinical trials falling outside the 90% prediction interval.

In addition, the predictive accuracy of the PBPK model was evaluated by comparing the clearance between the observed data and the simulated PBPK model on day 1 and at steady state following multiple daily dosing. The PK parameters were derived using noncompartmental analysis in Phoenix WinNonlin (version 7.0; Certara, St Louis, MO) for the observed data and for each individual from the simulated population data. Clearance following i.v. administration or apparent clearance after oral administration was calculated as dose/AUC_{0-24} using the linear log trapezoidal rule. The relative accuracy for clearance was calculated as a ratio of mean predicted values over mean observed values with a ratio for SD, as described previously[26–28]:

$$\sqrt{\left(\frac{\text{SD (observed)}}{\text{mean (observed)}}\right)^2+\left(\frac{\text{SD (predicted)}}{\text{mean (predicted)}}\right)^2} \times \frac{\text{mean (predicted)}}{\text{mean (observed)}}$$

We sought to evaluate whether CYP3A4 first-pass metabolism or P-gp efflux played a larger role in the model-derived bioavailability estimates for the 200–800 mg oral dosing regimens. We compared the bioavailability when CYP3A4 metabolism with TDI was included in the model without P-gp transport to estimates obtained when P-gp transport was included in the model without CYP3A4 metabolism with TDI.

Modeling the ELF compartment

In PK-Sim, for the small molecule model, there are four subcompartments within each tissue: blood cells, plasma, interstitial, and intracellular. The blood cells and plasma are both connected to arterial and venous blood and the interstitial compartment is connected to both plasma and the intracellular compartment. For the lungs, concentrations in these compartments using the default settings that assume passive distribution between compartments were less than that observed in ELF fluid from the clinical trial data. Because the mechanism for higher solithromycin concentrations into ELF is unknown, we created an ELF compartment in MoBi as an observer, which allows us to calculate ELF concentrations as a function of plasma concentrations without interfering with the mass balance equations. The concentrations in ELF were calculated using the equation: plasma concentration*$f_{u,p}$*ELF_ratio, where ELF_ratio is defined as the ratio of solithromycin concentrations in ELF to plasma concentrations. The mean ELF_ratio was determined to be 15 based on the observed concentration data in ELF and plasma from clinical trials, which was within the range (2.4–28.6) observed in clinical trials at steady state for the 400 mg daily dose in healthy volunteers.[8]

Table 2 Comparison of clearance values for solithromycin between the observed data and simulated PBPK model

	CL/F or CL on day 1, L/h					CL/F or CL after multiple doses, L/h				
	Observed data		PBPK model			Observed data		PBPK model		
Dosing regimen	Mean	SD	Mean	SD	Ratio	Mean	SD	Mean	SD	Ratio
200 mg p.o. daily	267	140	271	174	0.84	102	60	86	77	0.90
400 mg p.o. daily	103	141	218	152	3.23	96	198	57	54	1.34
600 mg p.o. daily	131	178	177	131	2.10	35	11	44	41	1.22
800 mg p.o. day 1, 400 mg p.o. days 2–5	61	54	146	106	2.78	32	13	53	49	1.67
400 mg i.v. daily	70	17	56	16	0.30	34	13	33	17	0.62
800 mg i.v. day 1	42	8	50	15	0.42	N/A	N/A	N/A	N/A	N/A

The ratio was calculated as the ratio of mean predicted values over mean observed values with a ratio for the SD described previously.[26–28]
CL, clearance; CL/F, clearance following oral administration; N/A, not applicable; PBPK, physiologically based pharmacokinetic model.

Assessment of target attainment rates in plasma and ELF

We calculated $AUC_{0–24}$/MIC ratios for ELF and unbound plasma concentrations (using a protein binding of 78%) for the following MIC values: 0.015, 0.03, 0.06, 0.125, 0.25, 0.5, and 1 μg/mL. We calculated target attainment rates by calculating the number of simulated subjects with an $AUC_{0–24}$/MIC ratio of 1.26 and 1.65 for bacterial stasis and 15.1 and 6.31 for a 1-$\log_{10}$ colony forming unit reduction, in ELF and unbound plasma, respectively.[9]

RESULTS

Model evaluation

After optimization, the PBPK model was able to describe the observed clinical trial data, including TDI and saturation of the CYP3A4 elimination pathway. Clearance decreased with increasing dose and time, and, consequently, $AUC_{0–24}$ increased with increasing doses and time (**Figure 1**). The clearance for the simulations and observations from clinical trials are shown in **Table 2**. In addition, the simulated bioavailability increased with dose, which is likely due primarily to CYP3A4 first-pass metabolism because the bioavailability ranged from 27%–28% if only P-gp transport was included in the model, but increased with dose from 60%–100% if only CYP3A4 metabolism with TDI was included in the model for the 200–800 mg oral doses. The bioavailability from the PBPK simulations correspond with typical values of bioavailability predicted using a Hill-type model in a previously performed population PK analysis: 50% vs. 40% for the PBPK model vs. the population PK model, respectively, for the 200 mg dose, 70% vs. 67% for the 400 mg dose, 78% vs. 76% for the 600 mg dose, and 72% vs. 80% for the 800 mg dose on day 1 (sponsor data (Cempra) on file).

We compared renal excretion of solithromycin between the simulated data and data obtained from a mass balance study performed in 8 healthy adult male subjects receiving a single 800 mg dose of (~100 μCi) of [^{14}C]-solithromycin administered i.v. After incorporating P-gp transport into the model, the fraction excreted unchanged in urine was 15% and 16% for the 800 mg dose after 24 and 48 hours, respectively, providing confirmation that the optimized K_m/V_{max} values for P-gp are reasonable; at least with respect to urinary excretion.

The plasma concentrations for solithromycin were highly variable in healthy adult subjects from clinical trials. For the i.v. data, 27% and 17% of observations were outside the 90% prediction window for the 400 mg daily and 800 mg single dose simulations, respectively (**Figure 2**). For the oral regimens, 5%, 20%, and 15% of observations fell outside the 90% prediction window for the 200 mg daily,

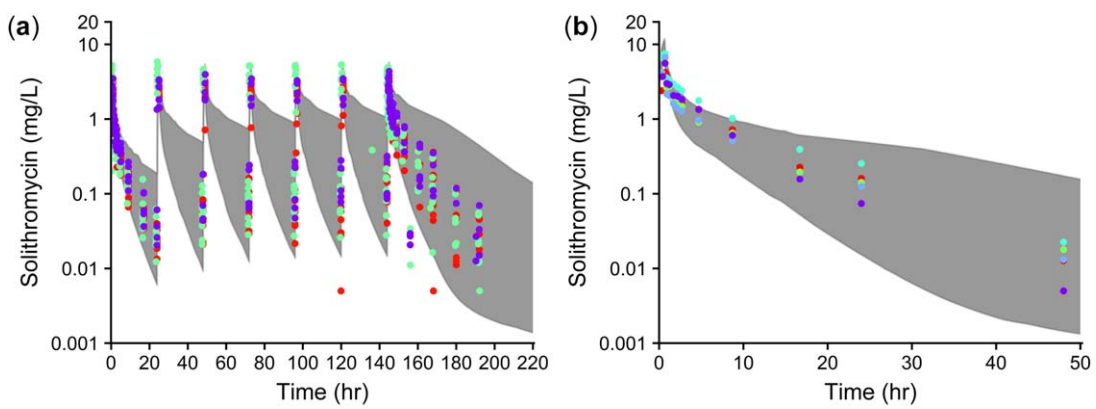

Figure 2 Population simulations for solithromycin plasma concentrations following 400 i.v. daily dosing (**a**) and an 800 mg i.v. single dose (**b**). The shaded area is the 5–95% range in concentrations from 100 simulated healthy adult subjects. The dots are the individual observations from clinical trials with each color reflecting concentrations for one individual, which differed between studies.

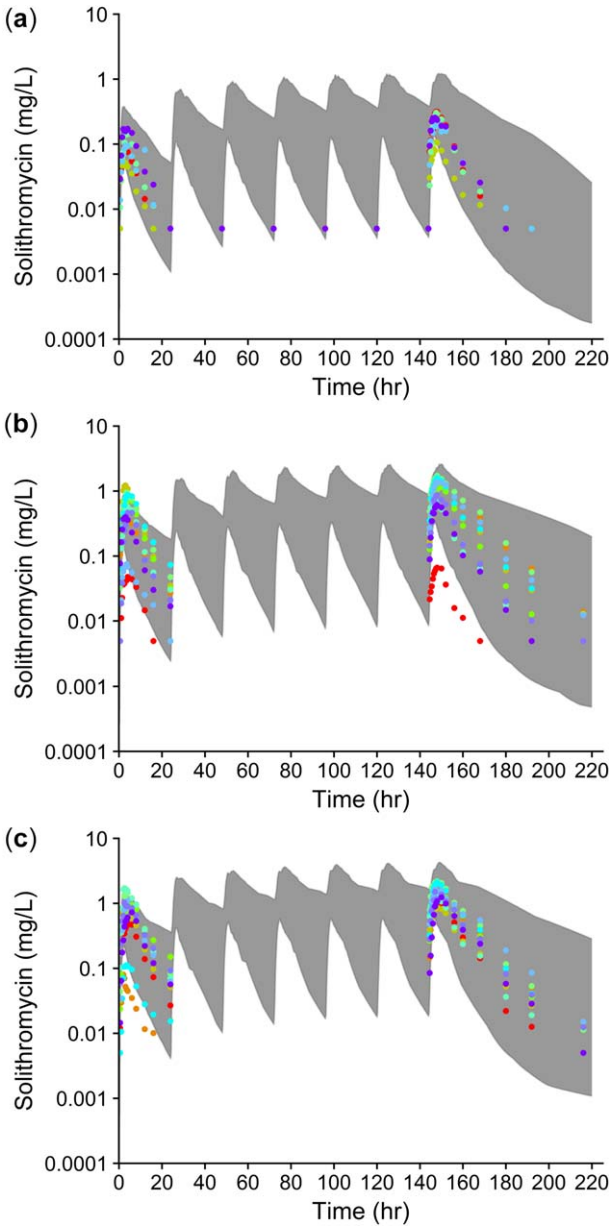

Figure 3 Population simulations for solithromycin plasma concentrations following 200 mg oral daily dosing (**a**), 400 mg oral daily dosing (**b**), and 600 mg oral daily dosing (**c**). The shaded area is the 5–95% range in concentrations from 100 simulated healthy adult subjects. The dots are the individual observations from clinical trials with each color reflecting concentrations for one individual, which differed between studies.

400 mg daily, and 600 mg daily simulations, respectively (**Figure 3**). For the oral regimen that demonstrated efficacy in phase III studies, 800 mg on day 1 followed by 400 mg once daily, there were 11% and 26% of observations from healthy adult subjects and patients with CABP, respectively, outside the 90% prediction interval (**Figure 4**). There were 23% of observations outside the 90% prediction interval for the ELF simulations (**Figure 5**). The prediction to observation ratios for clearance were calculated, and 17% and 100% of the estimates for the dosing regimens were within a 0.5–2.0 ratio window on day 1 and at steady state (day 5 or 7), respectively (**Table 2**).

Sensitivity analysis

Sensitivity analysis demonstrated that of all physicochemical parameters evaluated, lipophilicity and solubility reference pH had the largest impact on the simulated $AUC_{0–24}$ and C_{max} (**Supplementary Table S2**). All other parameters did not result in a $\geq$10% increase or decrease in $AUC_{0–24}$ and C_{max} when the parameter was increased 10% (**Supplementary Information S1 and Supplementary Table S2**).

Target attainment rates in plasma and ELF

For the 800 mg on day 1 followed by 400 mg on days 2–5 oral regimen, 100% of simulated adults achieved unbound $AUC_{0–24}$/MIC ratios associated with net-bacterial stasis in plasma for MICs between 0.015 and 0.125 μg/mL, and 97%, 88%, and 67% achieved unbound $AUC_{0–24}$/MIC ratios associated with net-bacterial stasis in plasma for MICs of 0.25, 0.5, and 1.0 μg/mL, respectively. The percentage of simulated healthy adults who achieved unbound $AUC_{0–24}$/MIC ratios associated with a 1-$\log_{10}$ colony forming unit reduction in plasma were 100% for MICs between 0.015 and 0.06 μg/mL, and 89%, 67%, 37%, and 11% for MICs of 0.125, 0.25, 0.5, and 1.0 μg/mL, respectively. In ELF, all simulated adults achieved $AUC_{0–24}$/MIC ratios associated with net bacterial stasis, and $\geq$97% achieved $AUC_{0–24}$/MIC ratios associated with a 1-$\log_{10}$ colony forming unit reduction for all MICs evaluated.

DISCUSSION

PBPK modeling is a powerful tool during drug development that can predict human drug concentrations based on preclinical data, estimate exposure in a target organ, and predict concentrations in patients with various ethnicities, ages, and disease states. A major advantage of PBPK modeling is that the dynamic flux of enzyme synthesis and degradation can be modeled to predict concentrations of parent and metabolite at any given time. PBPK modeling can also model TDI, defined as an increased potency of inhibition during *in vitro* incubation or during an *in vivo* dosing interval.[29] We optimized a whole-body PBPK model for adults, which incorporated time-dependent CYP3A4 auto-inhibition for solithromycin, a new fluoroketolide antibiotic in development for the treatment of CABP. This PBPK model can serve as a case study for other drugs in development that undergo TDI, accumulate in the lungs, and/or that have ample clinical trial data but limited *in vitro* data readily available. In addition, this adult model will provide a mechanistic structure from which to extrapolate solithromycin PK to different cohorts, such as children, where there is knowledge of the maturational processes responsible for solithromycin disposition and access to those parameters is accessible with PBPK modeling. Future research will include scaling this adult model to children to predict pediatric dosing.

Similar to other macrolide and ketolide antibiotics (telithromycin, clarithromycin, and erythromycin),[19,30–32] solithromycin undergoes mechanism-based inhibition of CYP3A4. Mechanism-based inhibition is a specific type of TDI in which

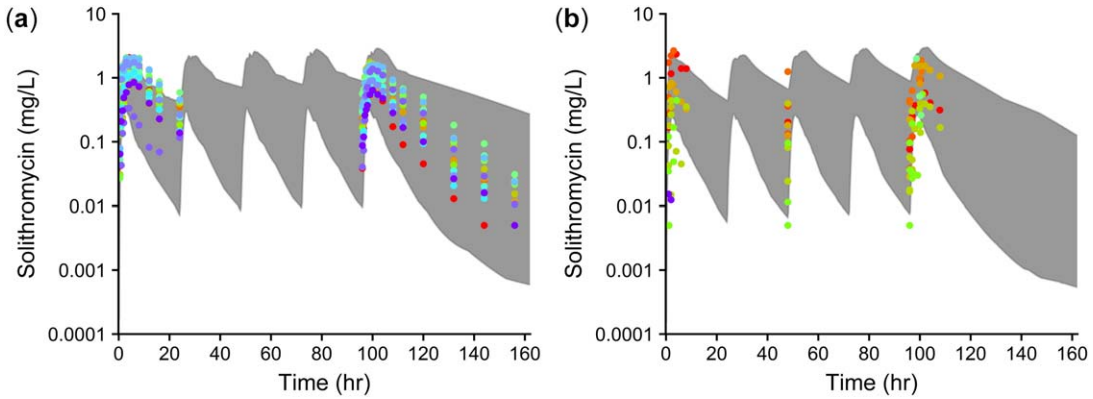

Figure 4 Population simulations for plasma concentrations for the 800 mg on day 1 followed by 400 mg orally daily regimen for the phase I population in healthy adults (**a**) and the phase II population in patients with community-acquired bacterial pneumonia (**b**). The shaded area is the 5–95% range in concentrations from 100 simulated subjects. The dots are the individual observations from clinical trials with each color reflecting concentrations for one individual, which differed between studies.

the enzyme is permanently inactivated by an inhibitory reactive metabolite thereby requiring enzyme synthesis for recovery.[29] Our PBPK model for solithromycin accurately captured TDI with AUC increasing as a function of dose and time. Nonlinear PK for solithromycin was observed in clinical trials and the simulated values of $AUC_{0–24}$ and clearance were comparable to the observed values obtained from clinical trials.[6,8] However, the model predictions were more accurate at steady state (days 5 or 7) compared to day 1, as measured by the values outside the 0.5–2.0 ratio window for the prediction to observation ratios for clearance, which incorporated the ratio for SD (**Table 2**). In particular, for the 400 mg, 600 mg, and 800 mg p.o. doses, the model is underpredicting $AUC_{0–24}$ and overpredicting apparent clearance on day 1. This might be because the K_I and K_{inact} were set at experimental values, which influences the values of the optimized parameters and may not allow P-gp or CYP3A4 catalytic efficiency (V_{max}/K_m ratios) to be globally accurate for all clinical data. Optimization of K_I and K_{inact} are not possible given their lack of identifiability when P-gp or CYP3A4 parameters are unknown.

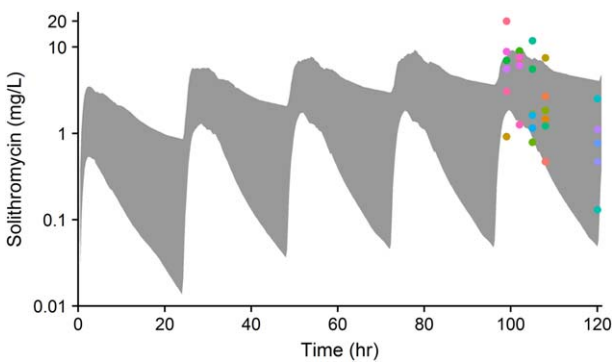

Figure 5 Population simulations for epithelial lining fluid solithromycin concentrations following 400 mg oral daily dosing. The shaded area is the 5–95% range in concentrations from 100 simulated healthy adult subjects. The dots are the individual observations from clinical trials with each color reflecting concentrations for one individual.

The PBPK model accurately captured dose-dependent bioavailability, which can be due to inhibition of P-gp efflux and/or inhibition of first-pass CYP3A4 metabolism in the gut and liver. The simulated mean absolute bioavailability for the 400 mg dose was 70% compared to the mean (range) of 62% (46–80%) for 5 subjects who received 400 mg i.v. and by mouth (capsules) of solithromycin (sponsor data (Cempra) on file). Previous studies evaluating the bioavailability of clarithromycin and telithromycin in rats demonstrated that the limited oral bioavailability is primarily due to low intestinal availability rather than first-pass metabolism in the liver.[33,34] In addition, grapefruit juice, a selective intestinal CYP3A4 inhibitor, did not significantly affect the oral absorption of clarithromycin or telithromycin.[35,36] These findings indicate that P-gp efflux in the intestinal epithelial cells plays a larger role than first-pass metabolism for the limited intestinal permeability.[34] However, the dose-dependent bioavailability for solithromycin in this model seems to be primarily due to CYP3A4 first-pass metabolism because changes in bioavailability with dose were more pronounced for CYP3A4 metabolism with TDI compared to P-gp transport alone.

The observed concentrations of solithromycin in ELF were greater than the predicted default lung plasma or interstitial fluid because no additional knowledge on the mechanisms responsible for lung accumulation were incorporated initially into the model. Several hypotheses have been proposed to explain these observed phenomena of higher ELF concentrations relative to plasma concentrations for macrolide antibiotics. Because these compounds are basic, they may accumulate in the acidic compartments of phagocytes within AM cells.[8] Supporting this assumption, a previously published PBPK model used sensitivity analysis to show that decreasing the pH in ELF may account for the underprediction of basic macrolide drugs in ELF.[37] The presence of drug transporters, such as P-gp, in the lung epithelial cells has also been postulated to cause increased distribution of macrolides into intrapulmonary fluid.[38,39] Finally, lysis of AM cells in the collected bronchoalveolar lavage fluid, and other technical errors in the measurement

of ELF, could also explain the higher concentrations in ELF relative to plasma.[38–40] Because the exact mechanism is currently unknown, we used an empiric approach by leveraging prior information from a phase I study[8] to calculate the ratio of ELF to plasma concentrations and incorporated it into the model. This method makes the least assumptions and is, thus, the most parsimonious model. Using this method, the variability in ELF concentrations was driven by the variability in both plasma concentrations and $f_{u,p}$. It seemed, based on the 23% of observations outside of the 90% prediction interval, that variability was slightly underpredicted and may be the result of additional variability in the process of ELF accumulation that could not be mechanistically accounted for.

High target attainments for simulated ELF concentrations suggests that the oral dosing regimen evaluated in clinical trials (800 mg on day 1, followed by 400 mg on days 2–5) is appropriate for the treatment of CABP. Similar findings were observed for a previously developed population-based PK model: net bacterial stasis and a 1-$\log_{10}$ colony forming unit reduction of $\geq$99.9% and 90.9%, respectively, for MIC values between 0.125 and 1 μg/mL.[41] Although PBPK and population-based PK modeling approaches are different, similar PK/PD relationships observed between the two models increases the confidence of our results.

This study had some important limitations. Important parameters that defined active transport and excretion were fixed to the extent possible and optimized when necessary. For example, CYP3A4 K_m was fixed to a value for another ketolide and may not be the value for solithromycin. This was performed to ensure that the parameters that were optimized were indeed identifiable and, thus, some model misparameterization very likely occurred as a result. Furthermore, model development utilized a parameter identification approach, using the observed data for both development and further validation. Finally, we used ratios of ELF to plasma concentrations from observed data to simulate the ELF concentrations because the exact mechanisms for higher concentrations into ELF are currently unknown. Further studies need to be performed to elucidate the mechanism for the high intrapulmonary concentrations of macrolides.

Acknowledgments. The authors thank Dr Huali Wu and Dr Anil Maharaj for providing technical assistance using the software PK-Sim.

Conflict of Interest. A.N.E. receives support for research from the National Institutes of Health (NIH) (1R01-HD076676-01A1; PI: Cohen-Wolkowiez). M.C.-W. receives support for research from the NIH (1R01-HD076676-01A1), the National Center for Advancing Translational Sciences of the NIH (UL1TR001117), the National Institute of Allergy and Infectious Disease (NIAID; HHSN272201500006I and HHSN272201300017I), NICHD (HHSN275201000003I), the Biomedical Advanced Research and Development Authority (BARDA) (HHSO100201300009C), and other sponsors for drug development in adults and children (www.dcri.duke.edu/research/coi.jsp). C.P.H. receives salary support for research from the National Center for Advancing Translational Sciences of the NIH (UL1TR001117). K.M.W. receives support from the Pediatric Critical Care and Trauma Scientist Development Program (5K12HD047349) and NICHD (1K23HD075891). B.D.J. is an employee of Cempra. D.G. receives support for research from NICHD (K23HD083465), the nonprofit organization Thrasher Research Fund (www.thrasherresearch.org), and from industry (Cempra and Jacobus Pharmaceutical Company) for drug development in adults and children. The remaining authors have no conflict of interest to disclose. The content is solely the responsibility of the authors and does not represent the official views of the NIH.

Source of Funding. This study was funded by the nonprofit organization Thrasher Research Fund (www.thrasherresearch.org) and the Eunice Kennedy Shriver National Institute of Child Health and Human Development (NICHD) (K23HD083465).

Author Contributions. S.S., A.E., M.C.-W., C.P.H., K.M.W., B.D.J., and D.G. wrote the manuscript. S.S., A.E., M.C.-W., and D.G. designed the research. S.S., A.E., M.C.-W., C.P.H., K.M.W., and D.G. performed the research. S.S. and A.E. analyzed the data.

1. Felmingham, D. *et al.* Surveillance of resistance in bacteria causing community-acquired respiratory tract infections. *Clin. Microbiol. Infect.* **8**(suppl. 2), 12–42 (2002).
2. The Center for Disease Dynamics, Economics & Policy (CDDEP). Antibiotic Resistance of Streptococcus pneumoniae in United States. <https://resistancemap.cddep.org/AntibioticResistance.php>. Accessed 29 September 2017.
3. Rodgers, W., Frazier, A.D. & Champney, W.S. Solithromycin inhibition of protein synthesis and ribosome biogenesis in Staphylococcus aureus, Streptococcus pneumoniae, and Haemophilus influenzae. *Antimicrob. Agents Chemother.* **57**, 1632–1637 (2013).
4. Barrera, C.M. *et al.* Efficacy and safety of oral solithromycin versus oral moxifloxacin for treatment of community-acquired bacterial pneumonia: a global, double-blind, multicentre, randomised, active-controlled, non-inferiority trial (SOLITAIRE-ORAL). *Lancet Infect. Dis.* **16**, 421–430 (2016).
5. File, T.M. Jr *et al.* SOLITAIRE-IV: a randomized, double-blind, multicenter study comparing the efficacy and safety of intravenous-to-oral solithromycin to intravenous-to-oral moxifloxacin for treatment of community-acquired bacterial pneumonia. *Clin. Infect. Dis.* **63**, 1007–1016 (2016).
6. Still, J.G. *et al.* Pharmacokinetics of solithromycin (CEM-101) after single or multiple oral doses and effects of food on single-dose bioavailability in healthy adult subjects. *Antimicrob. Agents Chemother.* **55**, 1997–2003 (2011).
7. Okusanya, O.O. *et al.* Population pharmacokinetic and pharmacokinetic-pharmacodynamic target attainment analysis for solithromycin to support intravenous dose selection in patients with community-acquired bacterial pneumonia. Interscience Conference on Antimicrobial Agents and Chemotherapy. Abstract #A-1269. <http://www.cempra.com/products/Solithromycin-cem-101> (2012). Accessed 3 March 2017.
8. Rodvold, K.A., Gotfried, M.H., Still, J.G., Clark, K. & Fernandes, P. Comparison of plasma, epithelial lining fluid, and alveolar macrophage concentrations of solithromycin (CEM-101) in healthy adult subjects. *Antimicrob. Agents Chemother.* **56**, 5076–5081 (2012).
9. Andes, D.R., Okusanya, O.O., Forrest, A., Bhavnani, S.M., Fernandes, P., & Ambrose, G.A. Pharmacokinetic-pharmacodynamic analysis of CEM-101 against Streptococcus pneumoniae using data from a murine lung infection model, Abstract A1–688. 50th Interscience Conference on Antimicrobial Agents and Chemotherapy. <www.cempra.com/common/pdf/abstracts/Ambrose%20sp%20murine%20lung.pdf> (2010). Accessed 3 March 2017.
10. Oldach, D. *et al.* Randomized, double-blind, multicenter phase 2 study comparing the efficacy and safety of oral solithromycin (CEM-101) to those of oral levofloxacin in the treatment of patients with community-acquired bacterial pneumonia. *Antimicrob. Agents Chemother.* **57**, 2526–2534 (2013).
11. Meyer, M., Schneckener, S., Ludewig, B., Kuepfer, L. & Lippert, J. Using expression data for quantification of active processes in physiologically based pharmacokinetic modeling. *Drug Metab. Dispos.* **40**, 892–901 (2012).
12. Mayhew, B.S., Jones, D.R. & Hall, S.D. An in vitro model for predicting in vivo inhibition of cytochrome P450 3A4 by metabolic intermediate complex formation. *Drug Metab. Dispos.* **28**, 1031–1037 (2000).
13. Rowland Yeo, K., Walsky, R.L., Jamei, M., Rostami-Hodjegan, A. & Tucker, G.T. Prediction of time-dependent CYP3A4 drug-drug interactions by physiologically based pharmacokinetic modelling: impact of inactivation parameters and enzyme turnover. *Eur. J. Pharm. Sci.* **43**, 160–173 (2011).
14. Pichard, L., Fabre, I., Daujat, M., Domergue, J., Joyeux, H., & Maurel, P. Effect of corticosteroids on the expression of cytochromes P450 and on cyclosporin A oxidase activity in primary cultures of human hepatocytes. *Mol. Pharmacol.* **41**, 1047–1055 (1992).

15. Greenblatt, D.J. *et al.* Time course of recovery of cytochrome p450 3A function after single doses of grapefruit juice. *Clin. Pharmacol. Ther.* **74**, 121–129 (2003).
16. Lilja, J.J., Kivistö, K.T., Backman, J.T. & Neuvonen, P.J. Effect of grapefruit juice dose on grapefruit juice-triazolam interaction: repeated consumption prolongs triazolam half-life. *Eur. J. Clin. Pharmacol.* **56**, 411–415 (2000).
17. Lundahl, J., Regårdh, C.G., Edgar, B. & Johnsson, G. Relationship between time of intake of grapefruit juice and its effect on pharmacokinetics and pharmacodynamics of felodipine in healthy subjects. *Eur. J. Clin. Pharmacol.* **49**, 61–67 (1995).
18. Takanaga, H. *et al.* Pharmacokinetic analysis of felodipine-grapefruit juice interaction based on an irreversible enzyme inhibition model. *Br. J. Clin. Pharmacol.* **49**, 49–58 (2000).
19. Vieira, M.L. *et al.* Predicting drug interaction potential with a physiologically based pharmacokinetic model: a case study of telithromycin, a time-dependent CYP3A inhibitor. *Clin. Pharmacol. Ther.* **91**, 700–708 (2012).
20. Bayer Technology Services, Computational systems biology software suite. PK-Sim® and MOBI® manual. Version 6.3.2/6.3.2, SB Suite. <http://www.systems-biology.com/products/pk-sim.html>. Accessed 3 March 2017.
21. Berezhkovskiy, L.M. Volume of distribution at steady state for a linear pharmacokinetic system with peripheral elimination. *J. Pharm. Sci.* **93**, 1628–1640 (2004).
22. Barter, Z.E., Perrett, H.F., Yeo, K.R., Allorge, D., Lennard, M.S., & Rostami-Hodjegan, A. Determination of a quantitative relationship between hepatic CYP3A5*1/*3 and CYP3A4 expression for use in the prediction of metabolic clearance in virtual populations. *Biopharm. Drug Dispos.* **31**, 516–532 (2010).
23. Watkins, P.B., Wrighton, S.A., Schuetz, E.G., Maurel, P. & Guzelian, P.S. Macrolide antibiotics inhibit the degradation of the glucocorticoid-responsive cytochrome P-450p in rat hepatocytes in vivo and in primary monolayer culture. *J. Biol. Chem.* **261**, 6264–6271 (1986).
24. Yang, J. *et al.* Cytochrome p450 turnover: regulation of synthesis and degradation, methods for determining rates, and implications for the prediction of drug interactions. *Curr. Drug Metab.* **9**, 384–394 (2008).
25. Harwood, M.D., Neuhoff, S., Carlson, G.L., Warhurst, G. & Rostami-Hodjegan, A. Absolute abundance and function of intestinal drug transporters: a prerequisite for fully mechanistic in vitro-in vivo extrapolation of oral drug absorption. *Biopharm. Drug Dispos.* **34**, 2–28 (2013).
26. Jiang, X.L., Zhao, P., Barrett, J.S., Lesko, L.J. & Schmidt, S. Application of physiologically based pharmacokinetic modeling to predict acetaminophen metabolism and pharmacokinetics in children. *CPT Pharmacometrics Syst. Pharmacol.* **2**, e80 (2013).
27. Johnson, T.N., Zhou, D. & Bui, K.H. Development of physiologically based pharmacokinetic model to evaluate the relative systemic exposure to quetiapine after administration of IR and XR formulations to adults, children and adolescents. *Biopharm. Drug Dispos.* **35**, 341–352 (2014).
28. Zhou, W. *et al.* Predictive performance of physiologically based pharmacokinetic and population pharmacokinetic modeling of renally cleared drugs in children. *CPT Pharmacometrics Syst. Pharmacol.* **5**, 475–483 (2016).
29. Riley, R.J. & Wilson, C.E. Cytochrome P450 time-dependent inhibition and induction: advances in assays, risk analysis and modelling. *Expert Opin. Drug Metab. Toxicol.* **11**, 557–572 (2015).
30. Quinney, S.K., Zhang, X., Lucksiri, A., Gorski, J.C., Li, L. & Hall, S.D. Physiologically based pharmacokinetic model of mechanism-based inhibition of CYP3A by clarithromycin. *Drug Metab. Dispos.* **38**, 241–248 (2010).
31. Akiyoshi, T. *et al.* Mechanism-based inhibition profiles of erythromycin and clarithromycin with cytochrome P450 3A4 genetic variants. *Drug Metab. Pharmacokinet.* **28**, 411–415 (2013).
32. Zhang, X., Galinsky, R.E., Kimura, R.E., Quinney, S.K., Jones, D.R. & Hall, S.D. Inhibition of CYP3A by erythromycin: in vitro-in vivo correlation in rats. *Drug Metab. Dispos.* **38**, 61–72 (2010).
33. Padovan, J., Ralić, J., Letfus, V., Milić, A. & Bencetić Mihaljević, V. Investigating the barriers to bioavailability of macrolide antibiotics in the rat. *Eur. J. Drug Metab. Pharmacokinet.* **37**, 163–171 (2012).
34. Togami, K., Hayashi, Y., Chono, S. & Morimoto, K. Involvement of intestinal permeability in the oral absorption of clarithromycin and telithromycin. *Biopharm. Drug Dispos.* **35**, 321–329 (2014).
35. Shi, J., Montay, G., Leroy, B. & Bhargava, V.O. Effects of itraconazole or grapefruit juice on the pharmacokinetics of telithromycin. *Pharmacotherapy* **25**, 42–51 (2005).
36. Cheng, K.L., Nafziger, A.N., Peloquin, C.A. & Amsden, G.W. Effect of grapefruit juice on clarithromycin pharmacokinetics. *Antimicrob. Agents Chemother.* **42**, 927–929 (1998).
37. Gaohua, L. *et al.* Development of a multicompartment permeability-limited lung PBPK model and its application in predicting pulmonary pharmacokinetics of antituberculosis drugs. *CPT Pharmacometrics Syst. Pharmacol.* **4**, 605–613 (2015).
38. Togami, K., Chono, S. & Morimoto, K. Distribution characteristics of clarithromycin and azithromycin, macrolide antimicrobial agents used for treatment of respiratory infections, in lung epithelial lining fluid and alveolar macrophages. *Biopharm. Drug Dispos.* **32**, 389–397 (2011).
39. Peters, J. *et al.* Oral absorption of clarithromycin is nearly abolished by chronic comedication of rifampicin in foals. *Drug Metab. Dispos.* **39**, 1643–1649 (2011).
40. Kiem, S. & Schentag, J.J. Interpretation of antibiotic concentration ratios measured in epithelial lining fluid. *Antimicrob. Agents Chemother.* **52**, 24–36 (2008).
41. Okusanya, Ó.O., Bhavnani, S.M., Forrest, A., Fernandes, P. & Ambrose, P.G. Pharmacokinetic-pharmacodynamic target attainment analysis supporting solithromycin (CEM-101) phase 2 dose selection. Interscience Conference on Antimicrobial Agents and Chemotherapy. Abstract #A1–692. <http://www.cempra.com/common/pdf/Posters/00182_CEM_101_PKPD_TA_ICAAC10_A1_692_08sep10.pdf> (2010). Accessed 3 March 2017.

Supplementary information accompanies this paper on the *CPT: Pharmacometrics & Systems Pharmacology* website (http://psp-journal.com)